# Covalently Crosslinked Lipid Nanocapsule-Based Hydrogels Induces the Modern Drug Delivery Efficacy

Saba Niaz [1*], Guillaume Bastiat Partner [2], Patrick Saulnier [2]

## Abstract

Background: The integration of nanotechnology and hydrogel systems offers a promising strategy for localized drug delivery, particularly for hydrophilic and lipophilic drugs with sustained release. Nanoparticle-loaded hydrogels enhance drug pharmacokinetics and biodistribution, opening the door to novel administration routes. However, the potential of these hydrogels has been underutilized due to the reliance on conventional hydrogel architectures. Methods: This study focuses on developing polymer-free lipid nanocapsule (LNC)-based hydrogels using the Michael addition maleimide-thiol reaction to create stable networks. We characterized the viscoelastic properties of these hydrogels by varying LNC concentration, maleimide composition, crosslinker nature, and maleimide/SH molar ratio. Results: Our findings indicate that hydrogel stiffness is significantly influenced by the LNC concentration, maleimide composition, and the nature of the crosslinker. Furthermore, diffusion-based experiments demonstrated that the hydrogel dissolution rate is dependent on the SH PEG crosslinker, while the release behavior of model drugs is influenced by their molecular weight. Conclusion: The study suggests that polymer-free LNC-based hydrogels hold significant potential as drug delivery systems, offering controlled release and reduced toxicity. These findings pave the way for further exploration of novel hydrogel structures in drug administration.

**Keywords:** Lipid nanocapsules (LNCs), Hydrogels, Covalent crosslinking, Drug delivery systems, Michael addition reaction

***Significance*** | This study showed a novel covalently crosslinked hydrogel system, enhancing drug delivery via improved mechanical stability and controlled release.

*Correspondence. Saba Niaz, Imperial College London, UK.
E-mail: niazsaba274@gmail.com

Editor Md Shamsuddin Sultan Khan, And accepted by the Editorial Board Apr 08, 2024 (received for review Feb 05, 2024)

## 1. Introduction

Hydrogels are conventionally portrayed as three-dimensional architectures built through the non-covalent or covalent crosslinking of natural or synthetic hydrophilic polymers (Karvinen et al., 2019). Based on their physically- or chemically-networked conformation, hydrogels can adopt properties such as bioadhesiveness, biocompatibility, and biodegradability, becoming attractive biomaterials for medical purposes (Petros & Desimone, 2010; Shi, Votruba, Farokhzad, & Langer, 2010). In particular, the high tenability regarding the physicochemical properties explains their broad use in numerous applications, ranging from tissue engineering and regenerative medicine to drug delivery (Blanco, Shen, & Ferrari, 2015; Pitorre et al., 2017).

As a health technology, the use of hydrogel-based systems in the design of sustained-release formulations constitutes one of the first approaches for increasing the therapeutic window of active pharmaceutical ingredients (APIs) (Petros & Desimone, 2010; Shi et al., 2010). Their involvement in the pharmaceutical arsenal as a drug delivery platform has allowed the exploration and exploitation

**Author Affiliation.**
[1] Imperial College London, UK
[2] Université d'Angers, Inserm, CNRS, MINT, SFR ICAT, Angers, France

**Please cite this article:**
Saba Niaz, Guillaume Bastiat Partner et al. (2024). Covalently Crosslinked Lipid Nanocapsule-Based Hydrogels Induces the Modern Drug Delivery Efficacy, Biosensors and Nanotheranostics, 3(1), 1-10, 9800

of non-traditional drug administration routes (i.e., ocular (Kang-Mieler & Mieler, 2015), nasal (Karavasili & Fatouros, 2016), vaginal (Caramella, Rossi, Ferrari, Bonferoni, & Sandri, 2015), intestinal, intraarticular (Gerwin, Hops, & Lucke, 2006), intracerebral, and dermal administration (Cully, 2015)). Furthermore, through the development of painless and limited drug-administration-regime therapies, hydrogels have become pivotal in enhancing patient compliance and convenience (Petros & Desimone, 2010).

While hydrogel-based technologies can be harnessed in a vast number of health fields, their use in the development of nanomedicine-based treatments has gained a lot of attention (Pitorre et al., 2017; Shi et al., 2011). Nanomedicines, usually administered as suspensions by the intravenous route, are imperative for the improvement of API's therapeutic index by modulating the drug pharmacokinetics (PK) and biodistribution (i.e., stealthiness, passive/active targeting, reduced toxicity, among others) (Blanco et al., 2015; Pitorre et al., 2017). However, their pharmacological relevance is diminished when the scenario requires a localized drug administration (Pitorre et al., 2017). In the case of hydrogels, a drawback lies in the inability of being loaded with hydrophobic APIs due to their hydrophilic nature (Pitorre et al., 2017). Thus, the coupling of nano- and hydrogel technologies has appeared as a promising solution to overcome these limitations. Hybrid systems formed by dispersing non-viral nanocarriers (e.g., liposomes, micelles, nanocapsules (Wu et al., 2014), polymeric nanoparticles, dendrimers, etc.) in hydrogels can enable the local administration of hydrophilic and/or lipophilic drugs with a sustained release (Pitorre et al., 2017; Gazaille et al., 2021). Besides, the ability of these systems to mimic tissue viscoelastic and stiffness properties might pave the way for the development of drug delivery systems compatible with the intra-tissue administration (Wu et al., 2014). Such pharmacological relevance is evidenced by their harness in clinical research, including cancer therapy and the treatment of infectious/inflammatory diseases (Gazaille et al., 2021).

Regardless of the versatility in the possible conformations that nanoparticle-loaded hydrogel systems can be structured, their development has been restricted to the exploitation of conventional hydrogel architectures (Pitorre et al., 2017). Although the engineering of novel nanoparticle-loaded hydrogel designs might afford improvements in terms of drug PK and biodistributions, this approach has been limited to very few studies (Pitorre et al., 2017; Karvinen et al., 2019). In light of this, polymer-free lipid nanocapsule (LNC)-based hydrogel formulations have been recently developed for the sustained-release and local treatment of glioblastoma and lung cancer (Bastiancich et al., 2017; Pitorre et al., 2021). In these works, authors reported the assembling of hydrogel networks based on the direct binding of LNCs in suspension (Bastiancich et al., 2017; Pitorre et al., 2021). By decorating LNC shells with amphiphilic agents (e.g., lauroyl-gemcitabine (GemC12) or palmitoyl-cytidine (CytC16)), the researchers achieved inter-nanoparticular interactions through hydrogen bonds, leading to the manufacture of non-conventional hydrogels (Martinez-Jothar et al., 2018; Fu & Kao, 2011). As described, the main advantage of these novel drug delivery systems corresponds to the absence of components, such as polymers or gelling agents (Pitorre et al., 2021). This is especially important as toxicity related to hydrogel polymeric matrix is avoided and the degradation is exclusively influenced by the release of drug-loaded LNCs, differently from conventional hydrogel formulations (Pitorre et al., 2021).

Embracing the LNC-based hydrogels concept, we decided to explore the formulation of three-dimensional networks formed by the covalent association of LNCs. Coherently with the literature, we hypothesized that the covalent organization of nanoparticles might form architectures with attractive features in terms of mechanical strength (Martinez-Jothar et al., 2018; Fu & Kao, 2011). Moreover, given that the structural stability of non-covalently formed hydrogels depends on environmental conditions (i.e., pH, ion concentration, and temperature) (Martinez-Jothar et al., 2018), we anticipated that the covalent binding of LNC will build three-dimensional structures stabler than the above-mentioned LNC-based hydrogel systems (Martinez-Jothar et al., 2018).

We developed LNC-based hydrogels covalently crosslinked by the Michael addition maleimide-thiol reaction between maleimide-decorated LNCs (Maleimide-LNCs) and thiol (SH) polyethylene glycol (PEG) crosslinkers (Fu & Kao, 2011; Heurtault et al., 2002). Hydrogel formulations were designed using different SH PEG crosslinkers at various maleimide/SH molar ratios. Then, their structure was characterized through rheology- and diffusion-based methods. Finally, the viscoelastic and diffusion properties of the LNC-based hydrogels were evaluated as a function of LNC concentration, maleimide composition, crosslinker nature, and maleimide/SH molar ratio.

## 2. Materials and methods

### *2.1.Materials*:

Labrafac® WL1349 (caprylic–capric acid triglycerides) (Labrafac) was purchased from Gattefosse S.A. (Saint-Priest, France). Kollifor® HS15 (a mixture of 70:30 of polyethylene glycol 660 12-hydroxystearate and free polyethylene glycol 660) (Kol) was purchased from BASF (Ludwigshafen, Germany). Span® 80 (Span 80), 10X phosphate-buffered saline (10X PBS), polyethylene glycol dithiol (PEG dithiol) (Mn = 1.5, 3.4, and 8 kDa), and 4-arm polyethylene glycol thiol (4arm PEG SH) (Mn = 5, 10, and 20 kDa) were purchased from Sigma-Aldrich (Saint-Quentin-Fallavier, France). Sodium chloride (NaCl) was purchased from VWR International S.A.S. (Fontenay-sous-bois, France). Deionized water was obtained from a Milli-Q plus system (Millipore, Paris, France).

1,2-distearoyl-sn-glycero-3-phosphoethanolamine-N-[maleimide(polyethylene glycol)-2000] (DSPE-PEG-Maleimide) was purchased from Avanti Polar Lipids (Alabaster, USA). 1,1′-dioctadecyl-3,3,3′,3′-tetramethylindodicarbocyanine 4-chlorobenzenesulfonate (DiD), 3,3′-dioctadecyloxacarbocyanine perchlorate (DiO), and 5-carboxyfluorescein succinimidyl ester (5-FAM) were obtained from Invitrogen (Cergy-Pontoise, France).

***2.2 Formulation of lipid nanocapsules (LNCs):***

The formulation of LNCs was based on the phase-inversion temperature method (Perrier, Saulnier, Fouchet, Lautram, & Benoît, 2010; Shi, Kantoff, Wooster, & Farokhzad, 2017; Wong, Ashton, & Dodou, 2015). Briefly, the preparation of LNCs was attained after submitting an oil-in-water emulsion, composed of Labrafac (1.117 g), Kol (0.917 g), Span 80 (0.450 g), NaCl (0.054 g), and water (1.517 g), to three heating and cooling cycles between 90 °C and 50 °C, under a constant magnetic stirring (about 900 rpm). During the last cooling step, at 80 °C, the system was subjected to an irreversible thermal shock by adding 2 mL of cold water (4 °C), leading to the spontaneous forming of an LNC suspension. The LNC suspension was let in constant stirring until its temperature was reduced to room temperature before its further use.

For the formulation of Maleimide-LNCs, DSPE-PEG-Maleimide was inserted into the lipid nanocapsules through protocols consisting of the incorporation of this PEG-based phospholipid into the LNCs formulation during the last step of phase inversion process (Lorén et al., 2015).. For this strategy, different amounts of DSPE-PEG-Maleimide (5, 10, and 15 mg) were first solubilized in 0.5 mL of water to obtain concentrations ranging from 0.2% to 0.67% (w/wLNCs) in the final formulation. Right after the addition, 1.5 mL of water was added for the irreversible thermal shock step to conserve the concentration of nanoparticles equal to the conventional LNCs formulation. The concentration of the Maleimide-LNCs was adjusted as convenient by the simple addition of water to the final Maleimide-LNC suspension.

For the preparation of fluorescent-labeled LNCs (DiO or DiD-labelled LNCs), DiO or DiD was dissolved in a mixture of Labrafac and acetone at a concentration of 0.1% (w/wLabrafac). The acetone was removed from the mixture by its complete evaporation in a water bath (60 °C), under magnetic stirring. Then, the DiO or DiD-Labrafac was incorporated, along with the other ingredients, into the oil-in-water emulsion before initiating the LNCs formulation process, under dark conditions. LNC, DiO-labelled LNC, Maleimide-LNC, and DiD-labelled Maleimide-LNC suspensions were stored at 4 °C.

***2.3 Formulation of LNC-based hydrogels:***

LNC-based hydrogels were formulated via a thiol-maleimide Michael-type addition between Maleimide- LNCs and SH PEG crosslinkers (e.g., PEG dithiol and 4arm PEG SH) (Fu & Kao, 2011). LNC-based hydrogels were prepared by mixing a solution of one of the SH PEG crosslinkers (dissolved in water) and the Maleimide-LNC suspension (1/4 (vPEG thiol crosslinker/vMaleimide-LNCs)), with various -maleimide/-SH molar ratio (R = 0.125 to 4 (n/n)). The thiol-maleimide covalent reaction was allowed to proceed under constant shacking (about 650 rpm) for at least 3 hours at room temperature. LNC-based hydrogels were stored at 4 °C.

For the formulation of DiD-labelled LNC-based hydrogels containing DiO-labelled LNCs or 5-FAM, SH PEG crosslinkers were first dissolved in a DiO-labelled LNC suspension, or a 5-FAM aqueous solution (0.16 mg/mL). Then, the SH PEG crosslinker solutions were mixed with the DiD-labelled Maleimide- LNC suspension (1/4 (vPEG thiol crosslinker/vMaleimide-LNCs)), at an equimolar -maleimide/-SH ratio. DID-labeled LNC-based hydrogels, DiD-labelled LNC-based hydrogels containing DiO-labelled LNCs, and DiD- labelled LNC-based hydrogels containing 5-FAM were stored at 4 °C.

***2.4 Characterization of size distribution and zeta potential of LNCs:***

The hydrodynamic diameter (Z-ave), polydispersity index (PdI), and zeta potential (ZP) of LNC suspensions and Maleimide-LNC suspensions were characterized at 25 °C, using a Malvern Zetasizer® Nano ZS (Malvern Panalytical, Worcestershire, United Kingdom). The quasi-elastic light scattering instrument is equipped with a 4-mW Helium-Neon laser with an output wavelength of 633 nm and a scatter angle fixed at 173°. The correlation functions were fitted using an exponential fit (Cumulant approach) for the Z-ave and PdI determinations. The Smoluchowski approximation was used to determine the electrophoretic mobility required for ZP determination. For the measurements, the LNC suspensions were diluted in water at a LNC concentration of ~6 mg/mL. All characterizations were performed with similar conductivity values.

***2.5 Rheological properties of LNC-based hydrogels:***

The viscoelastic properties of the LNC-based hydrogels were measured at 20 °C after, at least, 12 hours of storage, using a Kinexus® rheometer (Malvern Panalytical, Worcestershire, United Kingdom) equipped with a cone plate geometry (diameter: 40 mm, angle: 2°). First, the linear regime of LNC-based hydrogels, expressed by the strain amplitude-independent elastic (G') and viscous (G") moduli, was characterized by oscillatory strain sweeps at a constant frequency of 1 Hz. Within this regime (0.1% constant oscillatory strain amplitude), G' and G" were measured as a function of the oscillatory frequency (from 0.1 to 10 Hz).

***2.6 Diffusion characterization in LNC-based hydrogels using the Fluorescence Recovery After Photobleaching (FRAP) technique:***

FRAP experiments were conducted on a Leica TCS SP8 AOBS confocal laser scanning microscope (Leica Microsystems, Wetzlar, Germany) equipped with an HC PL Fluotar 10x/NA 0.30 objective, using the FRAP module of LAS X software (v. 3.5.7.23225). LNC-based hydrogels (i.e., DiD-labelled LNC-based hydrogels, DiD-

labelled LNC-based hydrogels containing DiO-labelled LNCs, and DiD-labelled LNC-based hydrogels containing 5-FAM) and LNC suspensions (i.e., DiD-labelled Maleimide-LNC suspension, DiD-labelled Maleimide-LNCs suspension containing DiO-labelled LNCs, and a DiD- labeled Maleimide-LNCs suspension containing 5-FAM) were deposited on glass slides (75x26 mm) and analyzed at room temperature. The region of interest (ROI) for the bleach pulse was set in a 40 µm diameter circle, placed at the center of each image. The bleaching was achieved in a single step with the AOBS set at 100 % transmission for five lines from the Argon ion laser (458 nm (5 mW), 476 nm (4 mW), 488 nm (40 mW), 496 nm (6 mW) and 514 nm (10 mW)). DiO and 5-FAM were exited with the 488 nm line of an argon-ion laser (40 mW) while DiD was exited with the 633 nm laser line (10 mW) from a He-Ne laser. Fluorescence emission was detected from 492 to 550 nm for DiO and 5-FAM and from 637 to 750 nm for DiD. FRAP images were acquired with a 3.5x zoom factor. Post-bleach images were captured every two seconds for three minutes, 0.65 seconds after the bleaching sequence. The scan rate for the acquisition of pre-and post-bleach micrographs was 400 Hz. Finally, the FRAP data were stored as 512 pixel 12-bit tiff images with a pixel size of 0.65 µm2.

***2.7 Hydrogel degradation and drug release studies:***

LNC-based hydrogel disintegration and the release of model drugs (i.e., DiO-labelled LNCs or 5-FAM) from the LNC-based hydrogel were assessed in DiD-labelled LNC-based hydrogels containing DiO- labelled LNCs or 5-FAM. To this end, 4arm 20K SH or PEG dithiol 8K crosslinkers were first dissolved in a DiO-labelled LNC suspension, or a 5-FAM aqueous solution (0.16 mg/mL). Hydrogels (1 mL) were prepared by mixing DiD-labelled Maleimide-LNC suspensions with the SH PEG crosslinker solutions (1/4 (vPEG thiol crosslinker/vMaleimide-LNCs)) in hemolysis tubes (right edge, round bottom, 6 mL) (NAFVSM, France) at an equimolar -maleimide/-SH ratio. Then, the thiol-maleimide covalent reaction was allowed to proceed under constant shacking (about 650 rpm) for at least 3 hours at room temperature, under dark conditions. Following the hydrogel preparation, 4 mL of 1X PBS (pH 7.4, 37 °C) were carefully added to the hemolytic tubes without modifying the hydrogel shape. Subsequently, the tubes were sealed and incubated in dark conditions at 37 °C, under constant agitation for 6 days. At predetermined sampling times, 500 µL of the supernatants were collected and replaced with 500 µL of fresh medium (at 37 °C). The concentration of DiD-labelled LNCs, DiO-labelled LNC, or 5-FAM was determined by measuring the fluorescence intensity associated with each fluorophore (DiD, DiO, and 5-FAM) in the collected samples, using a FluoroMax®-4 (Horiba Scientific, New Jersey, USA). Excitation wavelengths were set to 648 nm for DiD and 440 nm for DiO and 5-FAM. Fluorescence emission spectra were collected from 653 to 800 nm for DiD and from 480 to 550 nm for DiO [505 nm] and 5-FAM [518 nm]. The cumulative release profiles of the DiD-labelled LNCs, DiO-labelled LNCs, or 5-FAM were obtained considering that 100% release corresponds to the fluorescence intensity measured for the complete disintegration of the LNC-based hydrogels.

***2.8 Statistics:***

Results are expressed as the mean ± standard deviation (SD) of at least three independent experiments. Statistical analyses were performed using GraphPad Prism (GraphPad Software, USA). Data were evaluated using the non-parametric Kruskal-Wallis statistical test, followed by the post-hoc Dunn test for pairwise comparisons. A p-value of $p < 0.05$ was considered statistically significant.

## 3. Results and discussion

***3.1 Design and rheology-based characterization of LNC-based hydrogels:***

This work aimed at the design and formulation of LNC-based hydrogels based on the association of LNCs. To that account, LNCs decorated with maleimide moieties (DSPE-PEG-Maleimide) were exposed to predetermined amounts of SH PEG crosslinkers to trigger the covalent reticulation of LNCs through the Michael addition thiol-maleimide reaction.

***3.1.1 Formulation of maleimide-decorated LNCs:***

Procedures for the maleimide decoration of LNCs were designed based on the formulation protocol of conventional (non-decorated) 50 nm-diameter LNCs, previously reported by Gazaille et al. Well-aligned with their work, LNC suspensions with a Z-average (Z-ave) around 50 nm and narrow size distribution (PdI < 0.1) were easily formulated in absence of DSPE-PEG-Maleimide as an excipient.

Maleimide insertion in the LNCs was then tacked by adding DSPE-PEG-Maleimide during last LNC formulation step (final concentrations = 0.2%, 0.45%, and 0.67% (w/wLNCs)). As presented in Table 1, size distributions of the formulated LNCs were statistically differentiated ($p < 0.05$) as a result of the LNCs preparation protocol; namely, after the addition of DSPE-PEG-Maleimide. The insertion of DSPE-PEG- Maleimide molecules in LNCs during the last cooling step of the formulations prompted the increase of the Z-ave and PdI of LNCs (from 22% to 35% and from 83% to 150%, respectively). Contrary, the ZP did not differentiate between the different types of LNCs.

As described by Perrier et al, such an increase in LNCs size distributions corresponds to the insertion of DSPE-PEG-Maleimide molecules into the surface of LNCs. However, the Z-ave increment in Maleimide-LNCs is lower than expected (about 90 nm), assuming a linear PEG chain conformation in the DSPE-PEG-Maleimide molecules (brush structure). Accordingly, DSPE-PEG-Maleimide molecules are likely arranged in a compact conformation (mushroom structure) throughout the surface of LNCs.

Following the maleimide decoration of LNCs, Maleimide-LNCs were mixed with predetermined amounts of SH PEG crosslinkers to trigger the covalent association of LNCs through the Michael addition thiol- maleimide reaction. Their influence of LNC concentration, maleimide composition, crosslinker nature, and -maleimide/-SH molar on the mechanical properties of LNC-based hydrogels were evaluated. To this end, the linear viscoelastic region (LVR) of LNC-based hydrogels was characterized by varying the oscillatory strain amplitude at a constant oscillation frequency of 1 Hz. All the analyzed hydrogels showed a linear behavior, corresponding to strain-independent elastic (G') and viscous (G") moduli, up to an oscillatory strain amplitude value of about 12%. Beyond the LVR, the G′ moduli decreased, implying the structure collapsed as a result of broad deformations.

***3.1.2 Influence of the LNC maleimide composition and concentration on the viscoelastic properties of LNC-based hydrogels:***

We evaluated the effects of maleimide composition in the hydrogel viscoelastic properties at LNC concentration of 100, 200, and 300 mg/mL. To this end, LNC-hydrogels were formulated by the equimolar -maleimide/-SH mixture of Maleimide-LNC suspensions (maleimide composition of 0.2 %,
0.45 %, and 0.67 % (w/wLNCs)) with 4arm PEG 10K SH crosslinker, and their mechanical properties were characterized.

As presented in Figure 1A, viscoelastic properties of LNC-based hydrogels were dependent on the maleimide composition in all the studied LNC concentrations. Increasing both formulation factors led to the increment of G' and G" moduli hydrogel values. Thus, LNC-based hydrogel formulation using an LNC concentration of 300 mg/mL and maleimide composition of 0.67 % (w/wLNCs) allowed the preparation of structures with the highest stiffness. On the other hand, at an LNC concentration of 100 mg/mL and maleimide composition of 0.2% (w/wLNCs), hydrogel formulations led to the obtaining of flowing viscous systems. A similar loss of the hydrogel structure due to the decrease of the LNC concentration occurred in LNC-based hydrogels formulated by auto-association of LNCs mediated by hydrogen bond interactions. In their research, the authors described the LNC concentration of 100 mg/mL as a lower limit, outside which gel hardness decreased in such a manner that hydrogels behave as gelatinous suspensions. The LNC concentration of 300 mg/mL and maleimide composition of 0.67% (w/wLNCs) were proved to be the formulation parameters that allowed the preparation of hydrogels with the highest rigidity, and they were kept constant in following LNC-based hydrogels formulations.

***3.1.3 Effects of the SH PEG crosslinker nature in the viscoelastic properties of LNC-based hydrogels:***

Next, the viscoelastic properties of LNC-based hydrogels were analyzed as a function of the nature of the SH PEG crosslinker used to trigger the LNCs' covalent reticulation. For these experiments, we formulated hydrogels using equimolar -maleimide/-SH amounts of two types of SH PEG crosslinkers: PEG dithiol (Mn = 1.5, 3.4, and 8 kDa) and 4arm PEG SH (Mn = 5, 10, and 20 kDa).

A gradual augmentation of the hydrogel G' and G" moduli values was observed as the SH PEG crosslinker number average molecular weight (Mn) increased (Figure 1B). The hydrogels with the stiffest structures were obtained at a crosslinker Mn of 8 kDa and 20 kDa for PEG dithiol and 4arm PEG SH crosslinkers, respectively. As explained by Summonte et al], such results might be supported by the influence of the structural characteristics (i.e., chain length and chain flexibility) of SH PEG crosslinkers. Alongside factors such as pH, pKa, or the presence of oxidizing agents, the crosslinker PEG chain length and chain flexibility play a pivotal role in the establishment of chemical interactions between compatible functional moieties, such as maleimide and thiol molecules [28]. In our scenario, the hydrogel rigidity increased by the use of longer SH PEG crosslinkers with higher flexibility. Supported by this reasoning, we decided to keep using PEG dithiol 8K and 4arm PEG 20K SH as SH PEG crosslinkers for the formulation of LNC-based hydrogels in all further experiments.

***3.1.4 Effects of the -maleimide/-SH molar ratio in the mechanical properties of LNC-based hydrogels:***

Our screening formulation parameters was completed by the assessment of the relationship between the - maleimide/-SH molar ratio with the mechanical properties of LNC-based hydrogels. We studied LNC- based hydrogels formulated by PEG dithiol 8K and 4arm PEG 20K SH crosslinkers at -maleimide/-SH molar ratios ranging from 0.125 to 4 (n/n).

As observed in Figure 1C, G' and G" moduli values varied in dependence on the formulation crosslinker density. The -maleimide/-SH molar ratio that allowed the preparation of hydrogels with higher stiffness was found to range between 0.5 and 1 (n/n) for both SH PEG crosslinkers. Particularly for the PEG dithiol 8K crosslinker, our results described the reduction of the hydrogel mechanical properties at - maleimide/-SH molar ratios lower than 0.5 (n/n) or higher than 1 (n/n), obtaining fragile structures at a - maleimide/-SH molar ratio of 0.125 and 2 (n/n). While similar effects in the hydrogel stiffness were observed while using the 4arm PEG 20K SH crosslinker, the loss of the hydrogel structure was resolved at -maleimide/-SH molar ratios higher than 1 (n/n). Indeed, regardless of the SH PEG crosslinker, the use of a -maleimide/-SH molar ratio of 4 (n/n) always resulted in the preparation of non-gelled structures. The reduction of the structure rigidity provoked by a decrease in the crosslinker concentration is also observed in conventional hydrogels (formed by the reticulation of polymers). As explained by Wong et al. (2015), the crosslinker density is a pivotal formulation factor that governs the hydrogel microstructure properties. If this factor increases, the interaction

**Table 1**. Size distributions (Z-average, Z-ave; and polydispersity index, PdI) and surface characteristics (Zeta potential, ZP) of LNCs as a function of maleimide composition: 0 %, 0.2 %, 0.45 %, and 0.67 % (w/wLNCs). Results were obtained by addition of DSPE-PEG-Maleimide at the last step of LNC formulations (mean ± SD; n = 4 - 13). Z-ave and PdI results obtained at the maleimide composition of 0 % (w/wLNCs) statistical differenced ($p < 0.05$) with the ones obtained at 0.2 % and 0.67 % (w/wLNCs).

| Maleimide composition (%) (*w/wLNC*) | Z-ave (nm) | PdI | ZP (mV) |
|---|---|---|---|
| 0 | 53 ± 2 | 0.06 ± 0.02 | -9 ± 2 |
| 0.2 | 71 ± 1 | 0.15 ± 0.01 | -8 ± 1 |
| 0.45 | 65 ± 3 | 0.11 ± 0.02 | -11 ± 2 |
| 0.67 | 71 ± 6 | 0.14 ± 0.03 | -9 ± 1 |

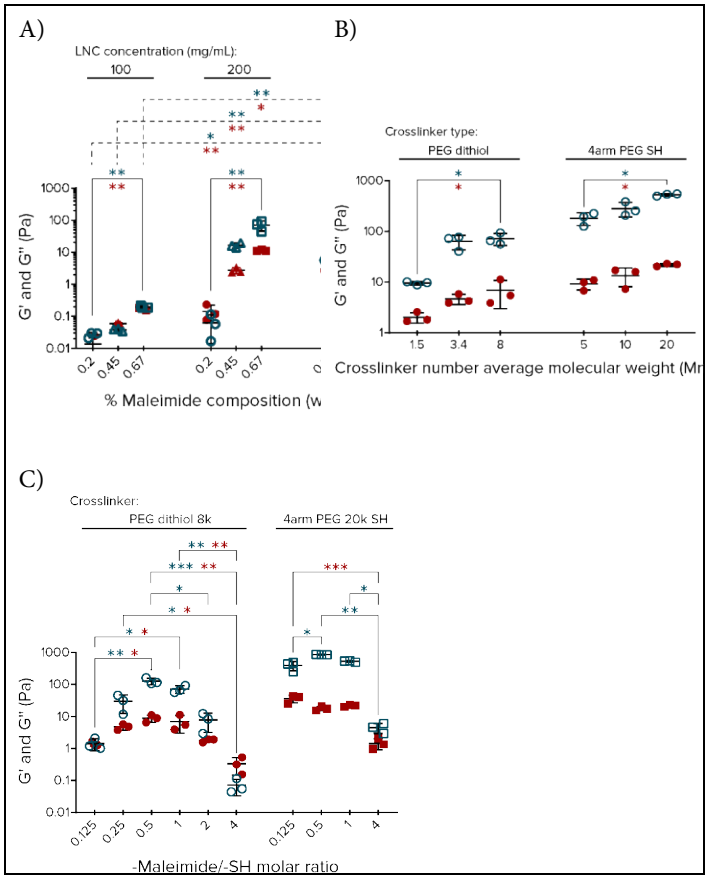


**Figure 1.** Rheological properties of LNC-based hydrogels: elastic (G') (blue hollow shapes: ○, Δ, and □) and viscous (G'') (red solid shapes: ●, ▲, and ▪ ) moduli of LNC-based hydrogels versus: A) maleimide composition (from 0.2% to 0.67% (w/wLNCs)) at different LNC concentrations (from 100 to 300 mg/mL) (SH PEG crosslinker = 4arm PEG 10K SH and -maleimide/-SH molar ratio = 1 (n/n)); B) SH PEG crosslinker nature (PEG dithiol (Mn = 1.5, 3.4, and 8 kDa) and 4arm PEG SH (Mn = 5, 10, and 20 kDa)) (maleimide composition = 6.7% (w/wLNCs); LNC concentration = 300 mg/mL; and -maleimide/-SH molar ratio = 1 (n/n)) ; and C) -maleimide/-SH molar ratio (from 0.125 to 4 (n/n) for PEG dithiol 8K and 4arm PEG 20K SH) (maleimide composition = 6.7% (w/wLNCs) and LNC concentration = 300 mg/mL). Oscillation frequency: 1 Hz, oscillatory strain amplitude: 0.1%, T = 20 °C (n = 3, mean ± SD). P-values are presented in blue (*) for G' and in red (*) for G'' moduli results (* $p < 0.05$, ** $p < 0.01$, *** $p < 0.001$).

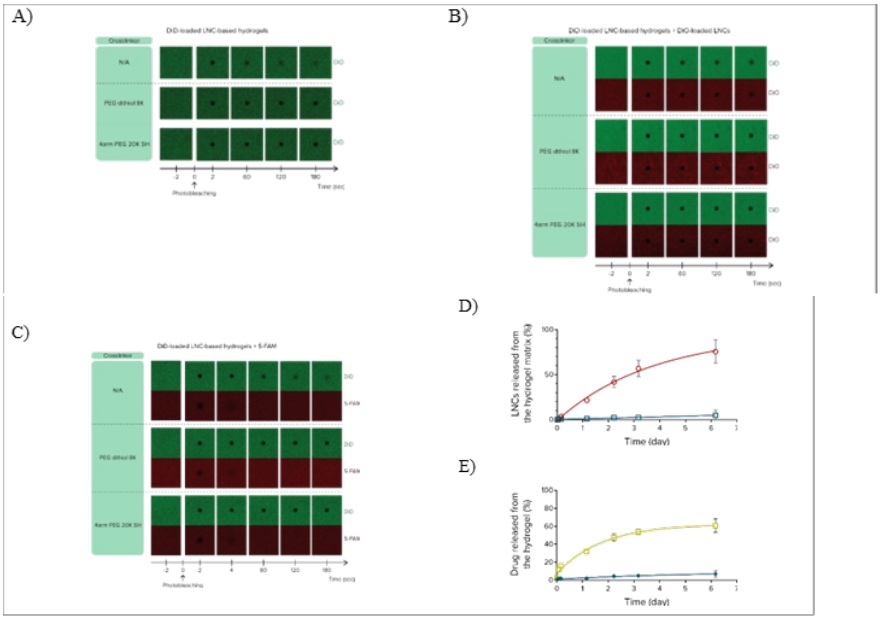


**Figure 2:** Diffusion experiments of LNC-based hydrogels (maleimide composition = 6.7% (*w/wLNCs*); LNC concentration = 300 mg/mL; SH PEG crosslinker = PEG dithiol 8K and 4arm PEG 20 K SH; and -maleimide/-SH molar ratio = 1 (*n/n*)). (A-C) FRAP micrographs of LNC-based hydrogels: A) DiD-labelled LNC-based hydrogels, B) DiD-labelled LNC-based hydrogels containing DiO-labelled LNCs, and C) DiD-labelled LNC-based hydrogels containing 5-FAM. Micrographs time-lapse corresponds to the different image acquisitions performed during the pre-and post-bleach phases of the FRAP experiment. (D and E) *In vitro* release of LNC-based hydrogels: D) Disintegration of LNC-based hydrogel (SH PEG crosslinker = PEG dithiol 8K (red profile) and 4arm PEG 20 K SH (blue profile)) and E) cumulative release of DiO-labelled LNCs (blue profile) or 5-FAM (green profile) from LNC-based hydrogels (SH PEG crosslinker = 4arm PEG 20 K SH). Release studies were performed in 1X PBS (pH 7.4) at 37 °C, under constant stirring, over six days. The release of DiD-labelled LNCs, DiO-labelled LNCs, and 5-FAM was quantified by fluorescence measurements (n = 3-6, mean ± SD).

and further reticulation between adjacent crosslinking junctions is facilitated; thus, forming denser hydrogel architectures (Zhou, Li, Zhang, & Wang, 2021).

Within our context, the degree of reticulation between LNCs in our LNC-based hydrogels is mediated by the SH PEG crosslinkers. Coherently, the more available thiol molecules (-maleimide/-SH molar ratio of Rheological properties of LNC-based hydrogels: elastic (G') (blue hollow shapes: ○, Δ, and □) and viscous (G") (red solid shapes: ●, ▲, and ▪ ) moduli of LNC-based hydrogels versus: A) maleimide composition (from 0.2% to 0.67% (w/wLNCs)) at different LNC concentrations (from 100 to 300 mg/mL) (SH PEG crosslinker = 4arm PEG 10K SH and -maleimide/-SH molar

### *3.2 Study of the diffusion properties of LNC-based hydrogels:*

#### *3.2.1 Hydrogel diffusion analyses by the FRAP technique:*

LNC-based hydrogels were submitted to FRAP evaluations to confirm the structuring of the hydrogel architecture by the stable covalent networking of Maleimide-LNCs and to observe the hydrogel matrix permeability behavior of model drugs with different molecular weights (MW) (50 nm-diameter DiO- labelled LNCs: high MW and 5 FAM: low MW). In this context, three fluorescence-labeled LNCs-based hydrogel formulations: DiD-labelled LNC-based hydrogels, DiD-labelled LNC-based hydrogels containing DiO-labelled LNCs, and DiD-labelled LNC-based hydrogels containing 5-FAM, were analyzed. Then, their diffusion results were contrasted with control samples, consisting of the identical LNC-based hydrogel formulations; however, in absence of SH PEG crosslinkers.

As presented in FRAP micrographs (Figure 2A-C), all the control samples showed a rapid recovery of DiD fluorescence (associated with DiD-labelled Maleimide-LNCs) after photobleaching, indicating the normal Brownian movement of non-reticulated Maleimide-LNCs in an aqueous suspension. When SH PEG crosslinkers participated in the LNC-based hydrogel formulation, the change of the Maleimide- LNCs diffusivity become evident, indicating the pivotal role of the SH PEG crosslinkers during the hydrogel building. Furthermore, as DiD fluorescence of LNC-based hydrogels formulated by PEG dithiol 8K or 4arm PEG 20K SH crosslinkers remained invariable over 180 seconds post-photobleaching, we inferred that the hydrogel matrix is constituted by a stable covalent association of Maleimide-LNCs.

Regarding the assessment of the permeation ability of model drugs, FRAP results revealed a weight- dependent drug diffusion behavior regardless of the crosslinker used for the hydrogel preparation. LNC- based hydrogels restrained the diffusion of our high MW drug model (Figure 2B). Contrary, 5-FAM fluorescence exhibited an immediate post-photobleaching fluorescence recovery (Figure 2C), implying the ability of our low MW drugs to easily infiltrate LNC-based hydrogels.

#### *3.2.2 LNC-based hydrogel disintegration and drugs release assessments:*

We performed in vitro release studies to analyze the hydrogel matrix disintegration rate (Maleimide-LNC release) and the release of the model drugs into 1X PBS at 37 °C, under constant agitation. The disintegration rate of hydrogels was tracked in DiD-labelled LNC-based hydrogels formulated by PEG. dithiol 8K or 4arm PEG 20K SH crosslinkers while the release profile analysis of model drugs was exclusively conducted in DiD-labelled LNC-based hydrogels formulated by 4 arm PEG 20K SH.

During the hydrogel disintegration evaluations (Figure 2D), we observed the progressive dissolution of LNC-based hydrogels uniquely in formulations that employed the PEG dithiol 8K crosslinker. For this case, measurements of DiD fluorescence intensity displayed a hydrogel disintegration of 75 ± 13% (n = 6) after 6 days. On the other hand, the structure of LNC-based hydrogels formulated with 4arm PEG 20K SH was more resistant, showing a minimal disintegration of 5 ± 6% (n = 6) over the same time.

An explanation of the different disintegration rates found between hydrogels formulated with PEG dithiol 8K or 4arm PEG 20K SH might be rooted in the particular molecular structure of each crosslinker. While the PEG dithiol 8K is formed by a linear PEG chain with an SH functional group at each extreme, 4arm PEG 20K SH is arranged in a branched configuration that possesses four SH functional groups. Fundamentally, 4arm PEG 20K SH is able to bind with more than two adjacent LNC crosslinking junctions at a time, prompting a higher degree of crosslinking and forming denser hydrogel structures than PEG dithiol 8K.

Complementary with our FRAP observations, drug release studies showed distinct drug release profiles based on the drug MW (Figure 2E). Again, the 5-FAM showed a higher capacity to permeate the hydrogel matrix than DiO-labelled LNCs, reaching a cumulative release of 61 ± 7% (n = 3) and 7 ± 4 % (n = 3), respectively, over 6 days. A rapid release of low MW drugs from hydrogen bond-formed LNC- based hydrogels was witnessed by Pitorre et al. Nevertheless, they described the total liberation of fluorescein to occur in just a few hours, demonstrating that our LNC-based hydrogels formed by the covalent association of LNCs might have a higher ability to delay the release of low MW drugs. However, the understanding of the drug delivery platform behavior of these hydrogels needs to be completed by the drug release analysis of different molecules in a broader range of MW.

## 4 Conclusions and perspectives

Throughout this work, we presented the development of novel hydrogel structures constructed by the covalent reticulation of LNCs. In such endeavor, we achieved the reticulation of maleimide decorated LNCs, assisted by SH PEG crosslinkers, based on the

Michael addition maleimide-thiol reaction. We found that LNC concentration, maleimide composition, crosslinker nature, and -maleimide/-SH molar ratio are relevant for determining the hydrogel viscoelastic properties. In summary, the more rigid hydrogel networks were formulated at the higher LNC concentration and maleimide composition values. Likewise, hydrogel structure stiffness increased proportionally to the crosslinker Mn and when exposing the LNC crosslinking junctions to -maleimide/-SH equimolar amounts of crosslinker molecules. Complementary, our diffusion experiments revealed an SH PEG crosslinker-dependent hydrogel dissolution rate. Over 6 days of in vitro release conditions, hydrogels formulated by PEG dithiol 8K showed a nearly complete degradation while hydrogels formulated by 4arm PEG 20K SH remained almost intact. Our FRAP experiments complemented the observed hydrogel drug release profiles showing a low hydrogel diffusivity of high MW drugs and high permeability of low MW drugs.

Although further in vitro and in vivo studies (genotoxicity tests, oxidative stress assays, bio-persistence, carcinogenicity, and pharmacokinetic studies) are imperative to prove the compatibility of these LNC- based hydrogels in biological systems, these preliminary results showed our LNC-based hydrogels being promising platforms for biomedical purposes. LNC-based hydrogels may be endowed with mechanical properties that can be adapted depending on the medical context. In this sense, LNC-based hydrogels formulated by the 4arm PEG 20K SH crosslinker have shown features such as a high resistance in aqueous media, which is needed for the development of long-term implants. However, while LNC-based hydrogels appear to control the release of drugs in a sustained long-lasting manner, the assessment of different drugs in a broader range of MW is needed to acquire a complete understanding of the behavior of these systems as drug delivery platforms.

## Author contributions

S.N. formulated the study objectives, constructed the hypotheses, and contributed to the manuscript revision. G.B.P. conducted the literature review and was involved in the data analysis. P.S. collected the data and wrote the results and conclusion sections. All authors reviewed and approved the final manuscript.

## Acknowledgment

Author was grateful to their department.

## Competing financial interests

The authors have no conflict of interest.

## References

Bastiancich, C., Bianco, J., Vanvarenberg, K., Ucakar, B., Joudiou, N., Gallez, B., Bastiat, G., Préat, V., & Danhier, F. (2017). Injectable nanomedicine hydrogel for local chemotherapy of glioblastoma after surgical resection. Journal of Controlled Release, 264, 45–54. https://doi.org/10.1016/j.jconrel.2017.08.019

Blanco, E., Shen, H., & Ferrari, M. (2015). Principles of nanoparticle design for overcoming biological barriers to drug delivery. Nature Biotechnology, 33(9), 941–951. https://doi.org/10.1038/nbt.3330

Caramella, C.M., Rossi, S., Ferrari, F., Bonferoni, M.C., & Sandri, G. (2015). Mucoadhesive and thermogelling systems for vaginal drug delivery. Advanced Drug Delivery Reviews, 92, 39–52. https://doi.org/10.1016/j.addr.2015.02.001

Cully, M. (2015). Inflammatory diseases: Hydrogel drug delivery for inflammatory bowel disease. Nature Reviews Drug Discovery, 14(10), 678. https://doi.org/10.1038/nrd4744

Duan, Z., Zhu, M., Wang, Y., Xu, L., & Jiang, Y. (2018). The effect of particle size on the cellular uptake and in vivo distribution of nanocarriers. Journal of Nanobiotechnology, 16(1), 129. https://doi.org/10.1186/s12951-018-0477-1

Feng, Q., & Zhao, Y. (2019). The influence of pH and ionic strength on the stability of nanoparticles: The role of environmental conditions. Nanotechnology Reviews, 8(1), 1067–1084. https://doi.org/10.1515/ntrev-2019-0050

Fu, Y., & Kao, W.J. (2011). In situ forming poly(ethylene glycol)-based hydrogels via thiol-maleimide Michael-type addition. Journal of Biomedical Materials Research Part A, 98(2), 201–211. https://doi.org/10.1002/jbm.a.33106

Gazaille, C., Sicot, M., Akiki, M., Lautram, N., Dupont, A., Saulnier, P., Eyer, J., & Bastiat, G. (2021). Characterization of biological material adsorption to the surface of nanoparticles without a prior separation step: A case study of glioblastoma-targeting peptide and lipid nanocapsules. Pharmaceutical Research, 38(5), 681–691. https://doi.org/10.1007/s11095-021-03034-8

Gerwin, N., Hops, C., & Lucke, A. (2006). Intraarticular drug delivery in osteoarthritis. Advanced Drug Delivery Reviews, 58(2), 226–242. https://doi.org/10.1016/j.addr.2006.01.018

Heurtault, B., Saulnier, P., Pech, B., Proust, J.E., & Benoit, J.P. (2002). A novel phase inversion-based process for the preparation of lipid nanocarriers. Pharmaceutical Research, 19(6), 875–880. https://doi.org/10.1023/A:1016121319668

Kang-Mieler, J.J., & Mieler, W.F. (2015). Thermo-responsive hydrogels for ocular drug delivery. Developments in Ophthalmology, 55, 104–111. https://doi.org/10.1159/000434694

Karavasili, C., & Fatouros, D.G. (2016). Smart materials: In situ gel-forming systems for nasal delivery. Drug Discovery Today, 21(1), 157–166. https://doi.org/10.1016/j.drudis.2015.10.016

Karvinen, J., Ihalainen, T.O., Calejo, M.T., Jönkkäri, I., & Kellomäki, M. (2019). Characterization of the microstructure of hydrazone crosslinked polysaccharide-based hydrogels through rheological and diffusion studies. Materials Science and Engineering C, 94, 1056–1066. https://doi.org/10.1016/j.msec.2018.10.048

Lee, J.H., Nam, Y.S., & Lee, K.S. (2017). Thermo-responsive hydrogels for controlled drug release and their applications in cancer therapy. Journal of Biomedical Materials Research Part A, 105(5), 1253–1261. https://doi.org/10.1002/jbm.a.35960

Loren, N., Hagman, J.K., Jonasson, J., Deschout, H., Bernin, D., Cella-Zanacchi, F., Diaspro, A., McNally, J.G., & Ameloot, M. (2015). Fluorescence recovery after photobleaching in material and life sciences: Putting theory into practice. Quarterly Reviews of Biophysics, 48(4), 323–387. https://doi.org/10.1017/S0033583515000013

Lorén, N., Hagman, J.K., Jonasson, J., Deschout, H., Bernin, D., Cella-Zanacchi, F., Diaspro, A., McNally, J.G., & Ameloot, M. (2015). Fluorescence recovery after photobleaching in material and life sciences: Putting theory into practice. Quarterly Reviews of Biophysics, 48(4), 323–387. https://doi.org/10.1017/S0033583515000013

Martinez-Jothar, L., Doulkeridou, S., Schiffelers, R.M., Sastre Torano, S., Oliveira, S., van Nostrum, C.F., & Hennink, W.E. (2018). Insights into maleimide-thiol conjugation chemistry: Conditions for efficient surface functionalization of nanoparticles for receptor targeting. Journal of Controlled Release, 282, 101–109. https://doi.org/10.1016/j.jconrel.2018.03.002

Miller, M.A., & Nelson, D.J. (2020). Biodegradable and bioadhesive hydrogels for controlled release of bioactive compounds. Journal of Controlled Release, 328, 329–343. https://doi.org/10.1016/j.jconrel.2020.09.029

Perrier, T., Saulnier, P., Fouchet, F., Lautram, N., & Benoît, J.P. (2010). Post-insertion into Lipid NanoCapsules (LNCs): From experimental aspects to mechanisms. International Journal of Pharmaceutics, 396(1–2), 204–209. https://doi.org/10.1016/j.ijpharm.2010.06.019

Petros, R.A., & Desimone, J.M. (2010). Strategies in the design of nanoparticles for therapeutic applications. Nature Reviews Drug Discovery, 9(8), 615–627. https://doi.org/10.1038/nrd2591

Pitorre, M., Gazaille, C., Pham, L.T.T., Frankova, K., Béjaud, J., Lautram, N., Riou, J., Perrot, R., Geneviève, F., & Moal, V. (2021). Polymer-free hydrogel made of lipid nanocapsules, as a local drug delivery platform. Materials Science and Engineering C, 126, 112188. https://doi.org/10.1016/j.msec.2021.112188

Rupp, R., Rosenthal, S.L., & Stanberry, L.R. (2007). VivaGel™ (SPL7013 Gel): A candidate dendrimer-microbicide for the prevention of HIV and HSV infection. International Journal of Nanomedicine, 2(4), 561–566. https://doi.org/10.2147/IJN.S1232

Shen, M., Xu, Y.Y., Sun, Y., Duan, Y.R., & Han, B.S. (2015). Preparation of a thermosensitive gel composed of a mPEG-PLGA-PLL-cRGD nanodrug delivery system for pancreatic tumor therapy. ACS Applied Materials & Interfaces, 7(35), 20530–20537. https://doi.org/10.1021/acsami.5b06043

Shi, J., Farokhzad, O.C., Votruba, A.R., & Langer, R. (2010). Nanotechnology in drug delivery and tissue engineering: From discovery to applications. Nano Letters, 10(10), 3223–3230. https://doi.org/10.1021/nl102184c

Shi, J., Kantoff, P.W., Wooster, R., & Farokhzad, O.C. (2017). Cancer nanomedicine: Progress, challenges and opportunities. Nature Reviews Cancer, 17(1), 20–37. https://doi.org/10.1038/nrc.2016.108

Summonte, S., Racaniello, G.F., Lopedota, A., Denora, N., & Bernkop-Schnürch, A. (2021). Thiolated polymeric hydrogels for biomedical application: Cross-linking mechanisms. Journal of Controlled Release, 330, 470–482. https://doi.org/10.1016/j.jconrel.2020.12.037

Wong, R.S.H., Ashton, M., & Dodou, K. (2015). Effect of crosslinking agent concentration on the properties of unmedicated hydrogels. Pharmaceutics, 7(3), 305–319. https://doi.org/10.3390/pharmaceutics7030305

Wu, Z.X., Zou, X.Y., Yang, L.L., Lin, S., Fan, J., Yang, B., Sun, X.Y., Wan, Q., Chen, Y., & Fu, S.Z. (2014). Thermosensitive hydrogel used in dual drug delivery system with paclitaxel-loaded micelles for in situ treatment of lung cancer. Colloids and Surfaces B: Biointerfaces, 122, 90–98. https://doi.org/10.1016/j.colsurfb.2014.06.052

Zhou, Y., Li, Z., Zhang, Y., & Wang, H. (2021). A review of drug delivery systems for hydrophobic drugs: Nanocarriers and their applications. Journal of Nanobiotechnology, 19(1), 160. https://doi.org/10.1186/s12951-021-01092-8